JOURNAL OF VIROLOGY, July 1997, p. 5209–5217 Vol. 71, No. 7
0022-538X/97/$04.00+0

Plasma Membrane Targeting of Chimeric Intracisternal A-Type Particle Polyproteins Leads to Particle Release and Specific Activation of the Viral Proteinase

REINHOLD WELKER,[1] ALFRED JANETZKO,[2] AND HANS-GEORG KRÄUSSLICH[1]*

Heinrich-Pette-Institut für experimentelle Virologie und Immunologie an der Universität Hamburg, D-20251 Hamburg,[1] and Max-Planck-Institut für Zellbiologie, D-68562 Ladenburg,[2] Germany

Received 21 January 1997/Accepted 20 March 1997

Retrovirus morphogenesis involves assembly of structural Gag polyproteins with subsequent budding from the plasma membrane, followed by proteolytic cleavage by the viral proteinase (PR) and extracellular maturation to the infectious virion. Intracisternal A-type particles (IAPs) are defective retroviruses that assemble and bud at the membranes of the endoplasmic reticulum (ER), where they remain as immature particles consisting exclusively of uncleaved polyproteins. To analyze requirements for intracellular polyprotein transport and PR activation, we constructed deletion and substitution mutations in the IAP *gag* gene, including the putative ER-targeting signal. Mutant polyproteins were transported to various intracellular locations, including the nucleus, the cytoplasm, the ER, and the plasma membrane. Interestingly, assembly of capsid-like particle structures occurred at almost all sites. However, only those polyproteins transported to the plasma membrane were efficiently and specifically cleaved by viral PR, with cleavage occurring predominantly within the virus particle. Thus, at least in the experimental system presented here, retroviral particle assembly can occur at almost any location within the cell, while polyprotein processing and, consequently, virion maturation are confined to a specific cellular site. These results suggest that a factor restricted to the plasma membrane is required to trigger PR activation and maturation of infectious retroviruses.

Retrovirus morphogenesis requires transport of individual virion components to a specific site within the producer cell with subsequent assembly and release by budding from the plasma membrane. Extracellular infectious retroviruses are composed of an inner core (products of the *gag* gene) containing the RNA genome and the viral replication enzymes (products of the *pol* gene) enclosed in a host-derived lipid membrane with inserted viral glycoproteins (products of the *env* gene). Morphogenesis of any retrovirus depends on the morphopoietic function of the Gag proteins, while other components are not essential for particle formation but are necessary for infectivity. The structural components of the core and the replication enzymes are synthesized on cytosolic polysomes and are transported and assembled as polyprotein precursors (Gag and Gag-Pol). Polyprotein transport is dictated primarily by signals in the matrix (MA) region. This domain is localized at the inner layer of the viral envelope (7, 28, 29), and MA mutations in several retroviruses impair or abolish targeting (reviewed in reference 17). Moreover, fusion of MA or N-terminal segments thereof with targeting-defective Gag proteins or heterologous proteins lead to plasma membrane localization of chimeric proteins, at least in some cases (1, 10, 38, 39, 42).

Retroviruses are initially formed as immature, noninfectious particles containing a spherical, electron-dense core underneath the viral envelope with an electron-lucent interior (reviewed in reference 25). Maturation of the virion depends on polyprotein cleavage and yields conversion to the condensed core, which exhibits different shapes in individual retroviruses. Proteolytic cleavage of polyproteins into individual domains by the viral proteinase (PR) occurs predominantly in the nascent particle. Timely activation of proteolysis is a critical feature in retrovirus morphogenesis, since premature PR activation leads to cytoplasmic processing of polyproteins and loss of particle assembly (2, 15), while insufficient proteolytic activity leads to noninfectious virus particles that are probably defective in uncoating (12, 14, 16).

Originally, retroviruses were classified according to their morphological appearance and budding phenotype as observed by electron microscopy (reviewed in reference 25). In type B and D retroviruses, spherical cores are assembled in the cytoplasm and subsequently transported to the plasma membrane, where budding and maturation take place. Type C oncoviruses and lentiviruses, on the other hand, do not appear to assemble larger structures in the cytoplasm, and formation of their immature core occurs concomitant with budding at the plasma membrane. A peculiar class of retroviruses are the intracisternal A-type particles (IAPs) of rodent cells which assemble and bud into cisternae of the endoplasmic reticulum (ER), where they remain as immature (A-type) particles (reviewed in reference 19). Differences in the morphogenesis pathway may be caused by different requirements for assembly or may reflect targeting and accumulation of the polyprotein. The latter hypothesis is supported by the observation that a point mutation in the MA domain of Mason-Pfizer monkey virus converted its budding phenotype from type D to type C with no detrimental effect on particle yield (31). Redirection of budding was also observed for a large internal deletion mutation in the human immunodeficiency virus type 1 (HIV-1) MA domain removing 85 amino acids but leaving the signal for N-myristoylation intact (5, 6). In this case, immature particles were released into the ER, where they retained their spherical morphology. These results indicated that different pathways of retrovirus morphogenesis are related in principle and that maturation can depend on the site of virus formation.

* Corresponding author. Mailing address: Heinrich-Pette-Institut für experimentelle Virologie und Immunologie an der Universität Hamburg, Martinistr. 52, D-20251 Hamburg, Germany. Phone: 49 40 48051-241. Fax: 49 40 48051-184. E-mail: hgk@hpi.uni-hamburg.de.

Based on these observations, we reasoned that IAP polyproteins may be rescued to the plasma membrane by engrafting a heterologous targeting signal, leading to release of extracellular virus. In addition, altered targeting may also trigger polyprotein cleavage by IAP PR. Here, we report that a chimeric IAP polyprotein with its own targeting signal deleted but engrafted with the plasma membrane-targeting signal of the Src protein was indeed transported to the plasma membrane, leading to release of extracellular particles. Moreover, the chimeric polyprotein was specifically cleaved by the viral PR. This cleavage was not observed for other IAP-derived polyproteins localized to the cytoplasm or to the nucleus nor for polyproteins carrying a mutation in the PR active site.

MATERIALS AND METHODS

Expression plasmids. Plasmid pMIA10-1, containing the IAP genome MIA-14 (24), was kindly provided by K. Lueders. For expression of MIA-14 genes under the control of the cytomegalovirus (CMV) immediate-early (IE) promoter, the *Bst*EII-*Hin*dIII fragment from pMia10-1 (corresponding to nucleotides 342 to 6291 of the MIA-14 sequence) was filled in with Klenow enzyme and cloned into the *Sma*I site of plasmid pL31, which is a pUC18 derivative with the cloning sites flanked by the CMV IE promoter and the simian virus 40 poly(A) signal (kindly provided by M. Pawlita). The resulting plasmid was named pL-MIA-2. To replace the first 10 codons of the IAP *gag* gene with the membrane-targeting signal of the Src protein, a fragment containing the entire *gag-PR* region of the IAP genome was amplified by PCR (forward primer, 5′-GCGGATCCAGTAAGTC AAAGCCTAAAGATCTAGAAGCCCTTT-3′; reverse primer, 5′-GCAAGCT TACTAAGGAAAACCCAGACC-3′), cloned into pUC-HSRV-src through the newly introduced *Bam*HI and *Hin*dIII sites, and sequenced at the new 5′ end. The resulting plasmid (pUC-MIA-src) contains an optimized sequence for eukaryotic translation initiation, a *Nco*I site followed immediately by a *Bam*HI site, and the *src* membrane-targeting signal. To create pL-MIA-3, a *Kpn*I-*Eco*RI fragment (corresponding to nucleotides 594 to 960 of the IAP genome, including the modified 5′ terminus of the *gag* gene) from pUC-MIA-src was ligated with the *Eco*RI-*Hin*dIII fragment [corresponding to nucleotides 960 to 6291 of MIA-14 and the simian virus 40 t splice and poly(A) signal] and with the *Hin*dIII-*Kpn*I fragment of pL-MIA-2 (corresponding to the pUC18 backbone and the CMV IE promoter). pL-MIA-4 was generated by deleting the region between the newly introduced *Xba*I site following the *src* membrane-targeting signal and the naturally occurring *Xba*I site (at nucleotide 677 of MIA-14) in pUC-MIA-src and subsequent cloning into the CMV expression vector as described for pL-MIA-3. To generate pL-MIA-5, pUC-MIA-src was cleaved with *Nco*I and *Xba*I, treated with Klenow enzyme, religated, sequenced, and subsequently cloned into the CMV expression vector in the same manner as pL-MIA-3. For deletion of the MA-equivalent region, a fragment of *gag* was amplified by PCR starting at nucleotide 1231 of MIA-14 (forward primer, 5′-GCG GATCCGCTAGCATACAACAGGCATTTCCG-3′; reverse primer, same as above), cloned into pUC-HSRV-src (see above) through the newly introduced *Bam*HI and *Hin*dIII sites, and sequenced at the new 5′ end. This construct (pUC-MIA-ΔN) coded for an IAP Gag protein with a deletion from codons 2 to 222 and introduced four new codons at the site of truncation. A *Kpn*I-*Not*I (nucleotide 1915 of MIA-14) fragment from pUC-MIA-ΔN was ligated with the *Not*I-*Hin*dIII and *Hin*dIII-*Kpn*I fragments of pL-MIA-2 (see above) to generate pL-MIA6.

For in vitro transcription and translation of the IAP Gag polyprotein, a *Pst*I fragment corresponding to nucleotides 152 to 2555 of the MIA-14 genome was cloned into the *Pst*I site of pBluescript SK− (Stratagene) to allow transcription with T7 RNA polymerase (pBPstMIA). This plasmid encodes the complete MIA Gag polyprotein but does not contain the predicted active site of the putative MIA-14 PR. For expression of the putative IAP PR in *Escherichia coli*, a *Nco*I fragment corresponding to nucleotides 2356 to 3104 of MIA-14 was cloned into the *Nco*I site of pET16 (Novagen) to give plasmid pET-IAP;PR. To introduce an inactivating mutation into the active site of the putative IAP PR, a *Pst*I-*Hin*dIII fragment from pUC-MIA-src (nucleotide 2555 of MIA-14 to the end of *gag-PR*) was cloned into pBluescript (Stratagene). Site-directed mutagenesis was performed on a single-stranded DNA template by the method of Kunkel (20). The active-site mutation contains an aspartic-acid-to-alanine substitution at amino acid 705 of the IAP Gag-PR polyprotein (nucleotides 2676 to 2678 [GAT to GCT] of MIA-14). Subsequently, the mutation was inserted into the context of pL-MIA-2, pL-MIA-4, and the bacterial expression vector to give plasmids pL-MIA-2a, pL-MIA-4a, and pET-IAP;PRa, respectively.

Cells and transfections. COS-7 cells were maintained in Dulbecco modified Eagle medium supplemented with 10% heat-inactivated fetal calf serum, 100 U of penicillin per ml, 100 μg of streptomycin per ml, and 2 mM glutamine. Transfections were performed as described previously (23). Briefly, approximately 5×10^6 cells were suspended in 100 μl of phosphate-buffered saline (PBS) and electrotransfected with 20 μg of DNA by using a Bio-Rad gene pulser set at 150 V, 960 μF, and 100 Ω. For immunofluorescence analysis, cells growing on glass coverslips in tissue culture dishes were transfected with 10 μg of plasmid DNA by using the modified calcium phosphate method (4).

Immunofluorescence staining and microscopy. Cells grown on coverslips were fixed with methanol and acetone for 10 min each at −20°C and air dried. Fixed cells were incubated with rabbit anti-IAP Gag serum, which was raised against electrophoretically purified IAP Gag derived from mouse tumors (kindly provided by K. Lueders; 1:200 dilution in PBS–1% bovine serum albumin) and with fluorescein isothiocyanate-labeled anti-rabbit immunoglobulin G (IgG; 1:100; Dianova, Hamburg, Germany). For confocal laser scanning microscopy analysis, cells were fixed in 1% paraformaldehyde in PBS containing 1 mM magnesium chloride (PBS-Mg) at pH 7.2 for 8 min, permeabilized with freshly dissolved 0.1% saponin in PBS-Mg for 5 min, rinsed, and incubated for 10 min in PBS-Mg containing 100 mM glycine and subsequently with 1% bovine serum albumin (freshly dissolved) in PBS-Mg for 1 h at 37°C. Immunostaining was performed with rabbit anti-IAP Gag for 2 h and with fluorescein isothiocyanate-labeled anti-rabbit IgG for 1 h at 37°C in a moist chamber.

Electron microscopy. Electron microscopic analysis was performed as described previously (5). Briefly, transfected cells were grown as monolayers on overhead projection transparency sheets which had been washed with acetone and sterilized with ethanol. At 48 h after transfection, cells were fixed with 2.5% glutaraldehyde (Sigma) in 50 mM sodium cacodylate (pH 7.2) for 30 min at room temperature and embedded in 1% low-melting-point agarose in 50 mM sodium cacodylate (pH 7.2). The remaining steps were performed essentially as described by McDonald (22), except that the buffer used was 50 mM sodium cacodylate (pH 7.2), the cells were treated with 1% OsO_4 plus 0.8% $K_3Fe(CN_6)$ for 30 min at room temperature, and the preparations were dehydrated in a graded ethanol series. The cells were embedded in Epon by inverting filled BEEM capsules (Plano, Marburg, Germany) over the fixed and dehydrated cells which were still attached to the plastic sheets. Following polymerization at 60°C, ultrathin sections were cut with an LKB ultramicrotome and poststained with uranyl acetate and lead citrate. Sections were viewed and photographed on a Zeiss EM 902 electron microscope.

Bacterial expression of IAP PR. Single colonies of *E. coli* BL21 DE3 (36) freshly transformed with expression vectors pET-IAP;PR and pET-IAP;PRa were grown at 37°C in LB medium (35) supplemented with 100 μg of ampicillin per ml to an optical density at 600 nm of 0.6 and induced with 1 mM IPTG (isopropyl-β-D-thiogalactopyranoside) for 3 h. Bacteria were harvested, washed with PR buffer (see below), and analyzed for protein expression or lysed by sonication and used for cleavage of in vitro-translated Gag polyproteins (see below).

In vitro translation and PR assay. For in vitro transcription, pBPstMIA was linearized with *Bam*HI and incubated with T7 RNA polymerase for 4 h at 37°C in 80 mM *N*-2-hydroxyethylpiperazine-*N*′-2-ethanesulfonic acid (HEPES)-KOH (pH 7.7)–12 mM $MgCl_2$–40 mM dithiothreitol–2 mM spermidine containing 3 mM each ribonucleotide, ribonuclease inhibitor (Promega), and 5 U of yeast inorganic pyrophosphatase (Sigma) per ml. RNA was precipitated with 4 M LiCl, reprecipitated with ethanol, dissolved in water, and quantitated by photometric analysis. In vitro translation was performed with 250 μg of RNA per ml and 70% rabbit reticulocyte lysate (Promega) in the presence of a mixture of ^{35}S-labeled methionine and cysteine (specific activity, >1,000 Ci/mmol; PRO-MIX, Amersham). To assay for *trans*-cleavage activity of IAP PR, bacteria were lysed by sonication (see above) and incubated with 8 μl of in vitro-translated IAP Gag in 15 mM morpholineethanesulfonic acid (MES; pH 6.0)– 37 mM NaCl–0.75 mM EDTA–1.5 mM dithiothreitol (PR buffer) at 37°C for 2 h (18).

Analysis of protein products. For detection of extracellular virus particles, medium was cleared by filtration through a 0.45-μm-pore-size filter and centrifuged through a cushion of 20% (wt/vol) sucrose in PBS at 120,000 × *g* for 2 h at 4°C. For protein analysis, cell or particle extracts were separated on sodium dodecyl sulfate (SDS)-polyacrylamide gels containing 17.5% polyacrylamide (200:1 ratio of acrylamide to *N*,*N*-methylenebisacrylamide). For Western blot analysis, proteins were transferred to nitrocellulose membranes (Schleicher & Schuell) and reacted with rabbit polyclonal antiserum (1:5,000 dilution) raised against the IAP Gag protein (see above). Alkaline phosphatase-conjugated goat anti-rabbit IgG (Jackson Immunochemicals Inc.) was used as the second antiserum.

For analysis of bacterial expression products, gels were stained with 1% Coomassie blue R (Serva) by using standard methods (35). For detection of [^{35}S]methionine-labeled in vitro translation products, dried gels were exposed to Hypermax-β film (Amersham).

RESULTS

Subcellular localization of IAP-derived polyproteins. IAPs form by budding at the ER membrane and are retained in the ER as immature spherical enveloped particles. To determine whether targeting of IAP Gag polyproteins to different subcellular localizations can alter the site of particle formation, a panel of deletion and substitution mutants (Fig. 1) was constructed within the genome of the murine IAP MIA-14 (24). As a control, the wild-type MIA-14 coding region was inserted

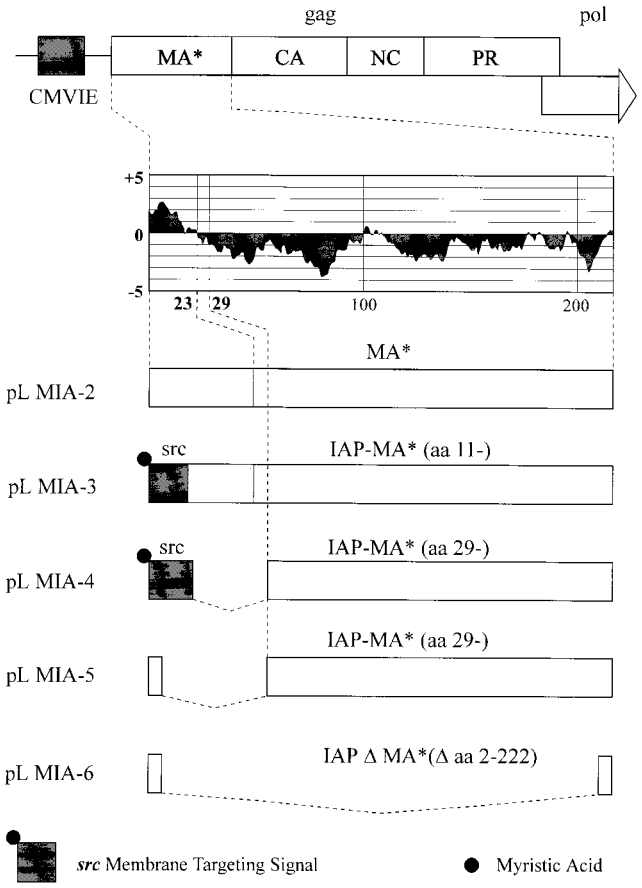

FIG. 1. Schematic representation of the IAP (MIA-14) genomic structure and various expression constructs. At the top, a relevant part of the *gag*-and-*pol* region within the IAP genome and the putative CA, NC, and PR domains are depicted as previously described (24). MA* indicates that an unrelated sequence is found as the N-terminal segment of the IAP polyprotein in the position of the retroviral MA domain (19). All constructs are expressed under control of the CMV IE promoter. Below, a hydrophobicity plot on a Kyte-Doolittle scale of −5 to +5 (positive numbers correspond to increased hydrophobicity) with a window size of 10 is depicted for the IAP MA* region. Below, the IAP MA* domain and the various mutants are expanded. pL-MIA-2 corresponds to the wild-type IAP sequence, which is not myristoylated at the N terminus but contains a stretch of hydrophobic amino acids (grey box). In pL-MIA-3, the first 10 codons of the IAP *gag* gene were replaced with the first 10 codons of the *src* gene (dark box), which contains a myristoylation signal (black circle). In pL-MIA-6, the entire MA* domain was deleted, except for the last five codons (giving rise to the amino acid sequence MGSASIQQAF.P, where P is the first predicted amino acid of CA). In plasmid pL-MIA-5, the first 28 codons of the IAP *gag* gene, including the hydrophobic region, were deleted, while in pL-MIA-4, the first 10 codons of *src* were substituted for these 28 codons of the IAP MA* region.

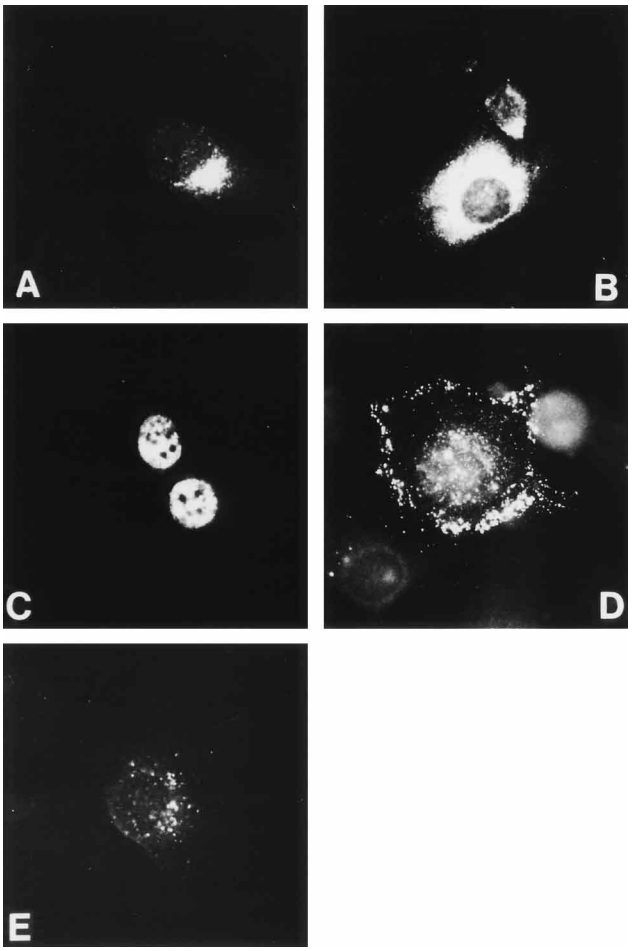

FIG. 2. Immunofluorescence analysis of COS cells transfected with the following plasmids: A, pL-MIA-2; B, pL-MIA-6; C, pL-MIA-5; D, pL-MIA-4; E, pL-MIA-3. Cells were harvested 48 h after transfection, fixed, and stained with polyclonal rabbit anti-IAP Gag serum.

into the same vector (MIA-2; Fig. 1). The N-terminal domain of MIA-14 Gag (equivalent to the MA domain of other retroviruses) contains a stretch of hydrophobic amino acids (12-ALLFLFTCYQVV-23; Fig. 1) which has been postulated to serve as an ER-targeting signal (24). Moreover, N-terminal protein sequence analysis performed on IAP Gag proteins purified from natural sources determined that arginine 27 is the first amino acid (21), suggesting that the very N-terminal domain of IAP Gag may be cleaved off after transport to the ER membrane. To test whether this signal and the MA-equivalent region of MIA-14 function as an ER-targeting signal, we constructed deletions of the entire MA-equivalent region (MIA-6) or of the hydrophobic N-terminal region (MIA-5). In addition, we replaced the N-terminal 10 codons of the *gag* coding region with the corresponding residues of the *src* coding region (MIA-3), which have been shown to serve as a dominant plasma membrane-targeting signal (27, 41) and therefore should override a putative ER-targeting signal of MIA-14. Finally, a construct with a deletion of the hydrophobic region and containing the *src* N-terminal region was made (MIA-4).

To analyze the subcellular localization of IAP-derived polyproteins, indirect immunofluorescence was performed on transiently transfected COS-7 cells. The wild-type IAP Gag polyprotein (MIA-2; Fig. 2A) revealed a perinuclear cap-like fluorescence, suggesting ER and Golgi localization. Electron microscopy analysis of MIA-2-transfected cells showed numerous retroviral particles budding into the cisternae of the ER and spherical immature particles within the ER (Fig. 3A) and occasionally in the perinuclear space (Fig. 3B). Thus, IAP polyprotein localization to the ER and its budding phenotype in rodent cells could be reproduced in monkey cells. Deletion of the entire MA-equivalent domain in the IAP Gag polyprotein (MIA-6, Fig. 2B) resulted in diffuse distribution of the antigen throughout the cytoplasm of transfected cells, indicating loss of subcellular targeting signals. A very different intracellular distribution of Gag was observed in MIA-5-transfected cells. Deletion of the N-terminal hydrophobic 28 codons of the MA-equivalent region (removing the putative ER-targeting signal) led to exclusively nuclear localization of Gag (Fig. 2C).

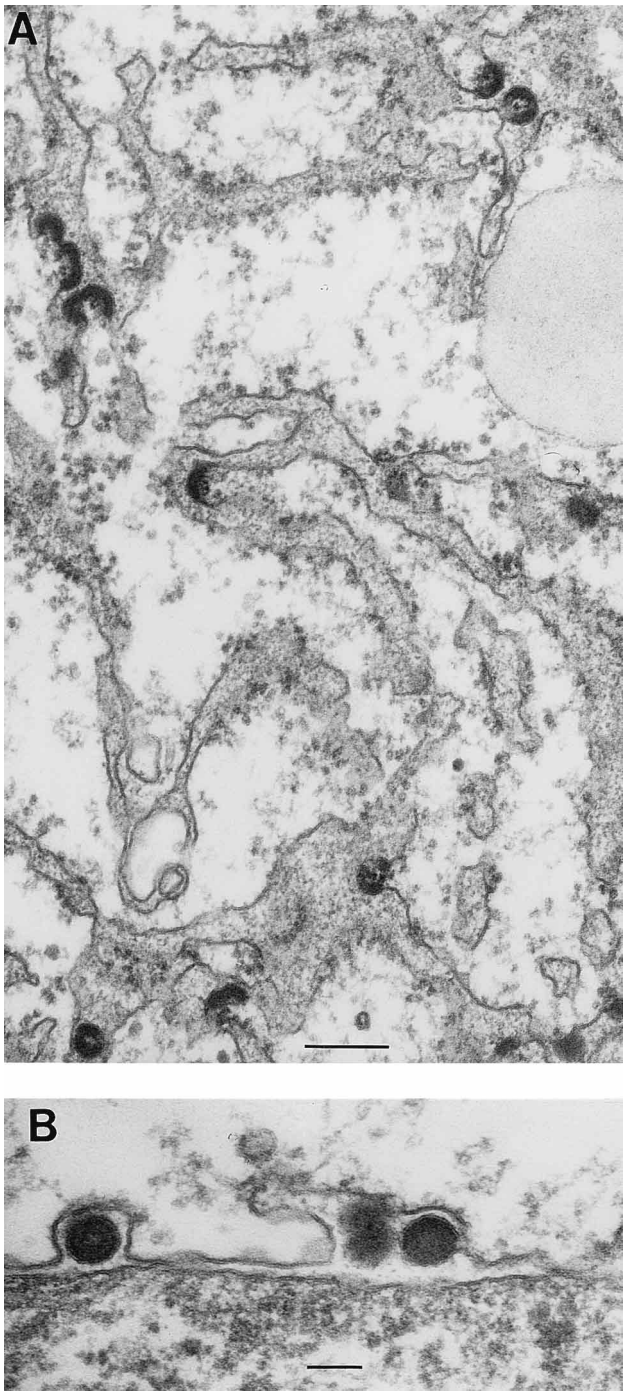

FIG. 3. Thin-section electron microscopy of COS-7 cells transfected with pL-MIA-2 at 48 h after transfection. (A and B) Electron-dense IAP particles budding into the cisternae of the ER and immature spherical particles within the ER (A) and perinuclear space (B). Bars, 200 (A) and 100 (B) nm.

Nuclear staining was diffuse with punctate spots and some unstained round areas. Interestingly, electron microscopy analysis of MIA-5-transfected cells revealed intranuclear accumulation of spherical particles that did not contain a lipid envelope (data not shown). Yet another intracellular localization was observed for MIA-4-derived polyproteins: grafting the plasma membrane-targeting signal of Src onto the N-terminally deleted IAP polyprotein yielded significant staining of the cellular periphery, indicative of efficient transport to the plasma membrane (Fig. 2D). In contrast, grafting the Src signal onto the wild-type IAP polyprotein (MIA-3, Fig. 2E) did not induce plasma membrane localization. Weak intracellular staining, most likely corresponding to cytoplasmic vesicles, was observed, and the chimeric polyprotein appeared unstable.

Plasma membrane targeting of chimeric polyproteins leads to rescue of extracellular particle formation. Since MIA-4-derived polyproteins showed a peripheral distribution of Gag polyproteins, it was of interest to analyze whether they were localized to the plasma membrane and whether release of extracellular particles could be observed. We performed electron microscopy analysis of MIA-4-transfected cells. Arrays of electron-dense structures budding from the plasma membrane were observed (Fig. 4A). Late budding structures (Fig. 4B, insert) showed the typical morphology of immature retroviral particles. In addition, extracellular immature particles were observed that were clearly separated from the producing cell (Fig. 4B). We also performed confocal laser scanning microscopy of paraformaldehyde-fixed, MIA-4-transfected cells, and these experiments also revealed predominant plasma membrane staining of the IAP Gag protein (see Fig. 7).

To analyze the stability of wild-type and chimeric polyproteins and their capacity to form particulate structures in the medium of transfected cells, we performed Western blot analysis of cells and particle extracts. Expression of the wild-type Gag polyprotein (MIA-2) yielded a single specifically immunoreactive band migrating with the previously described (24) molecular mass of approximately 70 kDa (Fig. 5, lane 2). A similar protein (albeit at lower abundance) was observed in MIA-3-transfected cells (Fig. 5, lane 3), while the deletion mutants yielded a slightly shorter (MIA-5 in Fig. 5, lane 5) or a considerably shorter (MIA-6 in Fig. 5, lane 4) polyprotein. No immunoreactive material was observed in the extracellular particle fraction in MIA-2-transfected cells (Fig. 5, lane 8) or in the other three mutants (MIA-3, -5, and -6; data not shown). A very different phenotype was observed for MIA-4-transfected cells. While mostly stable polyproteins were found in the other cases, cellular extracts from MIA-4-transfected cells yielded additional immunoreactive products besides the putative full-length polyprotein of approximately 70 kDa (Fig. 5, lane 6). These shorter products of approximately 35, 30, 24, and 20 kDa may correspond to proteolytic fragments of the chimeric polyprotein (see below). Similar immunoreactive proteins were observed in the particle fraction from the medium of MIA-4-transfected cells after centrifugation through a cushion of 20% sucrose (Fig. 5, lane 7). Proteins with equivalent electrophoretic mobility were stained in cell and particle extracts, but particles contained an increased amount of the shorter products, presumably at the expense of the full-length polyprotein. Thus, targeting of the chimeric MIA-4 Gag polyprotein to the plasma membrane led to release of extracellular particles and apparently induced proteolytic cleavage of the Gag polyprotein.

IAP PR is active in vitro. To analyze PR activity directly, we cloned a suitable restriction fragment containing the presumed PR region (based on known homologies with other retroviral and cellular aspartic PRs) into a bacterial expression vector. In addition, we constructed an active-site mutant PR by replacing the putative catalytic aspartic acid with an alanine codon. Bacterial extracts containing wild-type and mutant PRs were analyzed on Coomassie blue-stained gels (Fig. 6A). Expression of the mutant PR region yielded a product of approximately 27 kDa, in good agreement with the expected molecular mass of the protein encoded by the cloned fragment (239 amino acids

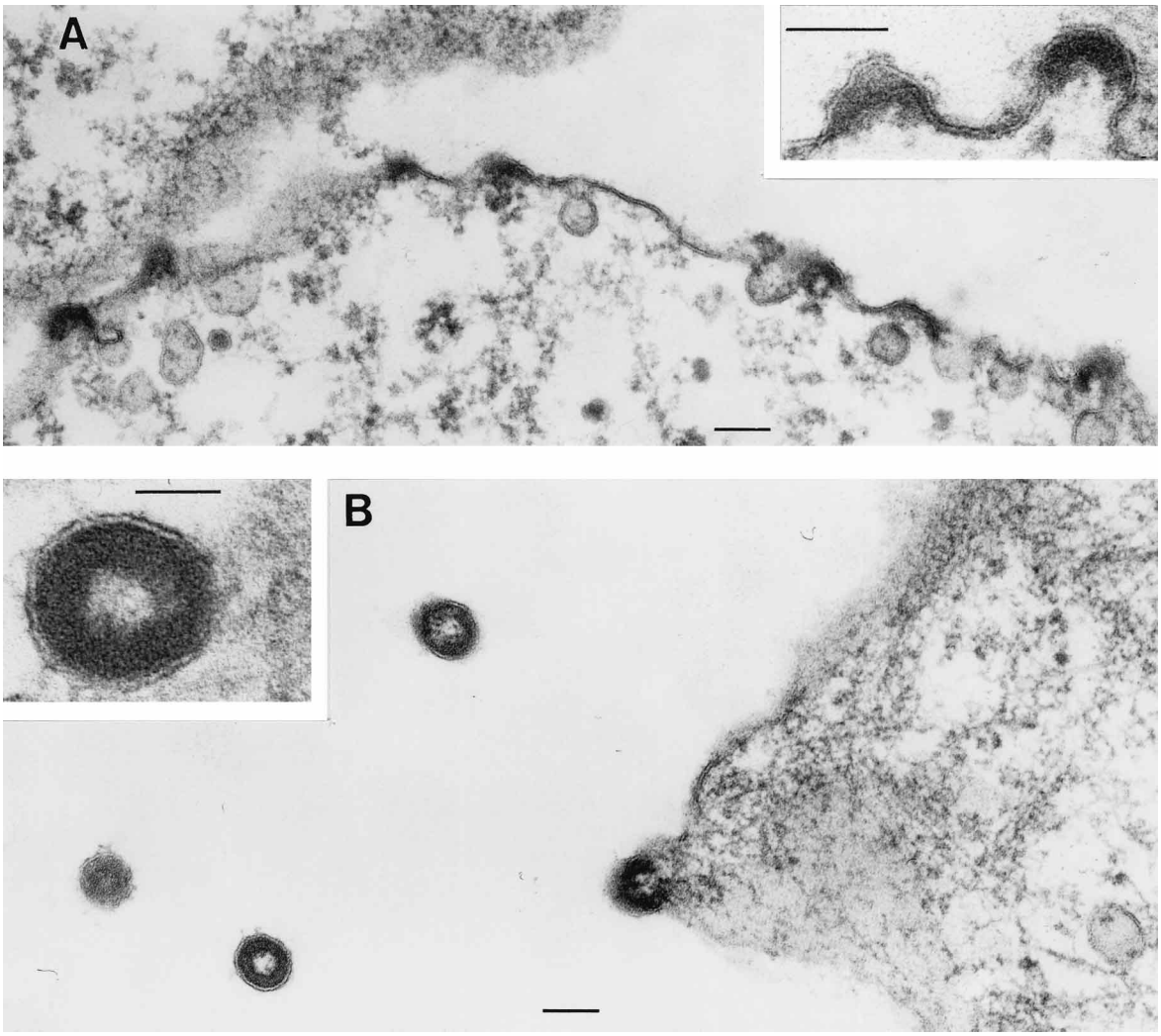

FIG. 4. Thin-section electron microscopy of COS-7 cells transfected with pL-MIA-4 at 48 h after transfection. (A and B) Electron-dense particles budding from the plasma membrane of transfected cells (A and insert) and late budding structures, as well as cell-released extracellular immature particles (B). Bars, 100 (A and B) and 50 (insert in B) nm.

or approximately 26 kDa). In contrast, expression of the wild-type region gave a major product of approximately 18 kDa, indicating that IAP PR is autocatalytically cleaved from a larger precursor to a product of 18 kDa.

To test the ability of bacterially expressed IAP PR to cleave the IAP Gag polyprotein in vitro, we performed in vitro transcription and translation of IAP Gag, followed by incubation with bacterial extracts containing active or inactive PR. In vitro translation revealed a major product of approximately 65 kDa (Fig. 6B, lane 2), while no labeled proteins were detected when RNA was omitted from the translation reaction (lane 1). Incubation of in vitro-translated IAP Gag polyprotein with increasing amounts of lysates from bacteria expressing wild-type PR under conditions known to be optimal for the activity of retroviral PRs led to gradual disappearance of the polyprotein with increasing production of shorter products of approximately 35, 24, and 20 kDa (Fig. 6B, lanes 3 to 6). These products were not observed when in vitro-translated Gag was incubated with bacteria expressing PR containing an active-site mutation (Fig. 6B, lanes 7 and 8) containing the PR coding region in reverse orientation (lane 9) or upon incubation in buffer only (lane 10). The three predominant cleavage products exhibited electrophoretic mobilities equivalent to those of the immunoreactive proteins observed in MIA-4-transfected cells and in the particle fraction derived from these cells (compare Fig. 4, lanes 6 and 7, and Fig. 6B, lane 6). In vitro cleavage was partially inhibited in the presence of specific inhibitors of retroviral PRs (e.g., Ro31-8959 [33]) but not by inhibitors of other proteases (data not shown).

IAP PR activity is triggered upon budding at the plasma membrane. Since IAP Gag polyproteins were cleaved by IAP PR and in vitro cleavage products were similar to those observed in MIA-4-derived particles, we analyzed whether IAP PR is indeed activated when chimeric polyproteins are assembled and bud from the plasma membrane. The active-site mutation was built into the MIA-4 context and, for control purposes, into the wild-type construct MIA-2. These plasmids were named pL-MIA-4a and pL-MIA-2a, respectively. Analysis of Gag protein localization by indirect immunofluorescence using confocal laser scanning microscopy revealed no significant difference in the intracellular distribution of Gag with or without an active PR (Fig. 7A). Immunoblot analysis of COS-7

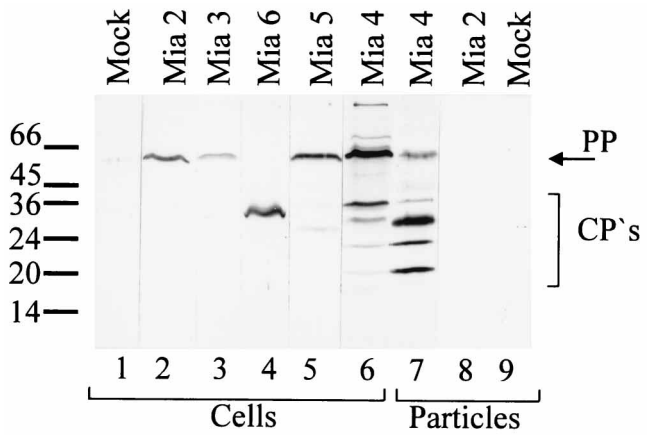

FIG. 5. Western blot analysis of *gag* gene products after transient transfection. At 48 h after transfection, cellular lysates (lanes 1 to 6) and extracellular particles (lanes 7 to 9) sedimented through a 20% sucrose cushion were resolved by SDS-polyacrylamide gel electrophoresis, and Western blots were probed with polyclonal rabbit anti-IAP Gag serum. The cells had been either mock transfected (lanes 1 and 9) or transfected with plasmid pL-MIA-2 (lanes 2 and 8), pL-MIA-3 (lane 3), pL-MIA-6 (lane 4), pL-MIA-5 (lane 5), or pL-MIA-4 (lanes 6 and 7). Molecular mass standards (in kilodaltons) are indicated on the left. The positions of the polyprotein (PP) and the putative cleavage products (CPs) are marked on the right.

cells transfected with the different expression vectors revealed no difference when the active-site mutation was present in the context of the wild-type polyprotein (Fig. 7B, lanes 1 and 2). In contrast, cleavage was abolished when the active-site mutation was introduced into the MIA-4-derived polyprotein (Fig. 7B, lanes 3 and 4). This difference was even more obvious when particle fractions from MIA-4- and MIA-4a-transfected cells were analyzed. Particles derived from MIA-4-transfected cells contained specifically immunoreactive proteins of 20, 24, and 35 kDa with little polyprotein remaining (Fig. 7B, lane 7). Particles derived from MIA-4a-transfected cells, on the other hand, contained no cleavage products, but only the uncleaved polyprotein (Fig. 7B, lane 8). An additional protein with a higher molecular mass observed in the particle fraction most likely corresponds to the IAP Gag-Pol precursor polyprotein (Fig. 7B, lane 8). In agreement with our previous results, no particles were detected in the culture medium of cells transfected with either MIA-2 or MIA-2a (Fig. 7B, lanes 5 and 6).

DISCUSSION

Morphogenesis of enveloped viruses is a stepwise mechanism which requires virion components to be transported to and concentrated at the assembly site. In many instances, additional extracellular maturation events are required to generate infectious virus which, in the case of retroviruses, involve proteolytic cleavage of the viral polyprotein with subsequent conformational reorganization of the spherical immature nucleocapsid to the condensed mature morphology. Mutational analysis of viral structural genes has allowed identification of regions important for transport and assembly. However, molecular mechanisms and cellular interacting partners involved in polyprotein transport, capsid assembly, budding, and maturation have been poorly defined to date. In particular, there is little information concerning the relationship of individual steps in the assembly pathway and their dependence on previous events. The results presented in this report indicate a coordinated interaction of viral and cellular factors in retrovirus morphogenesis and suggest that localization of the retroviral polyprotein may serve to trigger PR activation and subsequent maturation, which is a prerequisite for virion infectivity.

One can envision several possible routes for the transport of retroviral structural polyproteins. They may migrate through the cytoplasm by diffusion to be concentrated at the site of assembly, or they may associate with a cellular transport receptor directing them to a specific intracellular site. In either case, the Gag polyprotein should contain intrinsic information to specify the site of capsid assembly. This targeting signal resides in the MA domain at the N terminus of Gag in all of the cases analyzed, regardless of the retrovirus type (reviewed in reference 17). Apparently, morphogenesis of the various retrovirus types is similar in principle since conversion from a type

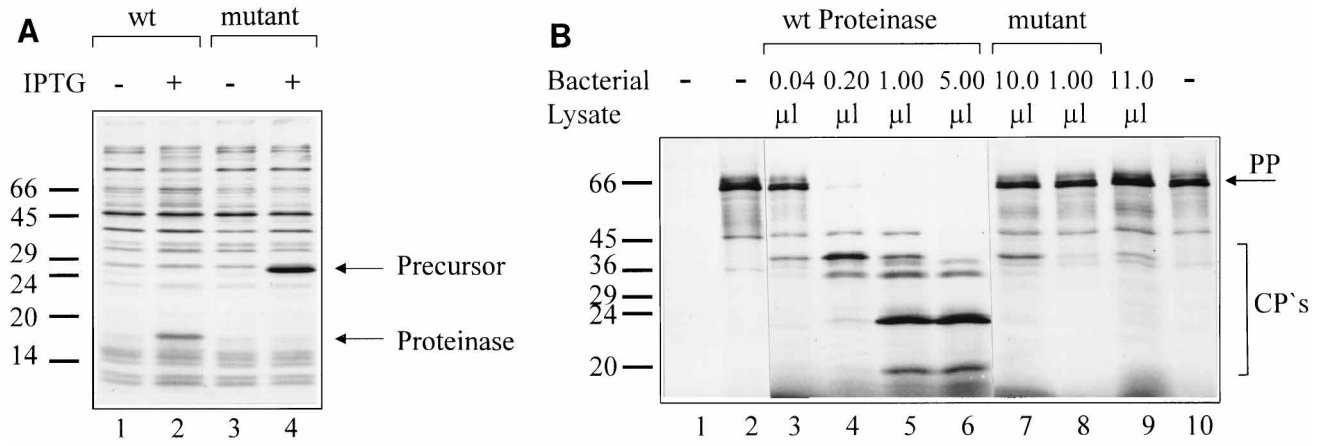

FIG. 6. (A) Expression of IAP PR in *E. coli*. Coomassie blue-stained SDS-polyacrylamide gel loaded with equal amounts of lysates from bacteria expressing either wild-type (wt; lanes 1 and 2) or mutant (lanes 3 and 4) IAP PR. Lysates from uninduced bacteria were loaded in lanes 1 and 3, and lysates from induced bacteria were in lanes 2 and 4. Molecular mass standards are indicated on the left, and the positions of the mutant PR precursor and PR itself are marked on the right. (B) In vitro cleavage of IAP Gag polyproteins by IAP PR. An IAP Gag polyprotein (truncated upstream of the PR active site) obtained by in vitro translation was either analyzed directly (lane 2) or incubated with cleavage buffer (lane 10) or with increasing amounts of lysates from bacteria harboring expression vectors for wild-type IAP PR (lanes 3 to 6), the active-site mutant thereof (lanes 7 and 8), or a plasmid containing the PR region in reverse orientation (lane 9). In the sample loaded in lane 1, no RNA was added to the translation reaction. The amount of bacterial lysate used in each cleavage reaction is indicated above each lane. Molecular mass standards are indicated on the left, and the positions of the polyprotein (PP) and the cleavage products (CPs) are marked on the right.

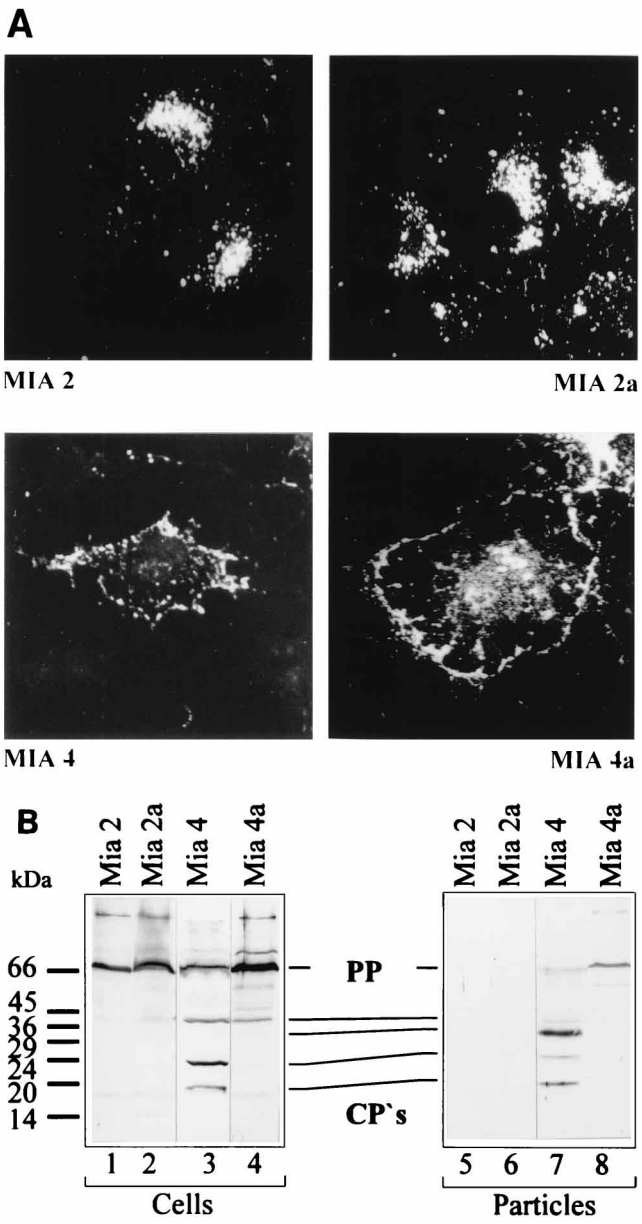

FIG. 7. (A) Confocal immunofluorescence analysis of COS-7 cells transfected with *gag-PR* expression vectors carrying either the wild-type *PR* sequence or that of an active-site mutant. Cells grown on glass coverslips were analyzed 48 h after transfection with the plasmids indicated below the panels. (B) Western blot analysis of COS-7 cells transfected with *gag-PR* expression vectors carrying either the wild-type *PR* sequence or that of an active-site mutant. At 48 h after transfection, cellular lysates (lanes 1 to 4) and extracellular particles (lanes 5 to 8) were analyzed by Western blotting. The cells had been transfected with plasmid pL-MIA-2 (lanes 1 and 5), pL-MIA2a (lanes 2 and 6), pL-MIA-4 (lanes 3 and 7), or pL-MIA-4a (lanes 4 and 8). Molecular mass standards are indicated on the left, and the positions of the polyprotein precursor (PP) and the cleavage products (CPs) are shown.

D to a type C virus can be achieved by a single point mutation in MA (31). Furthermore, assembly of immature spherical capsids of lentiviruses has been achieved in the cytoplasm provided the polyprotein concentration is sufficiently high, as in, e.g., baculovirus expression systems (8). Recent evidence indicates that retroviral capsid-like particles may also assemble inside bacteria (13) or even in a test tube (3, 34), provided their local concentrations are sufficiently high.

IAPs assemble and bud at the membranes of the ER, where they remain as immature particles and apparently never leave the cell (reviewed in reference 19). Sequence analysis of IAP genomes has indicated significant homology, in particular, with type D and B retroviruses (19, 26). Strikingly, homology ends upstream of the CA region of *gag* with no apparent homology in the 5′ portion of the IAP *gag* gene, which corresponds to the MA domain in other retroviruses. Thus, the IAP phenotype may be due to altered intracellular transport of structural polyproteins. In the present study, we have shown that ER transport of IAP polyproteins is governed by an N-terminal hydrophobic sequence (Fig. 1) and extracellular particle release may be rescued by replacing this targeting signal. Deletion of the hydrophobic sequence (MIA-5) led to nuclear transport of the polyprotein, possibly due to uncovering of a cryptic nuclear localization signal (NLS). This NLS must be contained within the MA-equivalent domain, since complete deletion of MA* yielded a cytoplasmically localized protein (MIA-6). Several candidate sequences resembling a canonical NLS were observed within the MA-equivalent region (e.g., amino acid 78-REIRRKRGKREKKK). Interestingly, mutant IAP polyproteins retained their ability to form capsid-like structures in the nucleus. Nuclear particles were nonenveloped, indicating that they assembled within the nucleus and did not bud through the nuclear membrane. Substitution of a dominant plasma membrane-targeting signal for the IAP ER localization sequence (MIA-4), on the other hand, led to accumulation of chimeric polyproteins at the plasma membrane with release of extracellular particles by budding from the cell surface. Substitution of the ER-targeting signal by various N-terminal segments of HIV-1 MA also led to particle release from the plasma membrane or yielded budding exclusively into the perinuclear space, depending on the length of the fragment used (40). These results support the conclusion that assembly of immature retrovirus particles can occur in various locations within a cell and is not dependent on specific intracellular sites or association with cellular membranes. Local concentration of the polyprotein, possibly in combination with nucleic acid association, appears to be the determining feature in capsid assembly.

In contrast, triggering of polyprotein cleavage and virion maturation may require additional factors and may be temporally and spatially regulated. From studies with HIV and type C retroviruses, it has become clear that PR activation has to occur within a narrow time window and therefore needs to be tightly controlled. Premature PR activation as well as incomplete cleavage led to loss of retroviral infectivity (reviewed in reference 37). Delayed triggering of proteolysis is most obvious in the case of type B and D viruses, where assembly and budding are distinct and uncoupled reactions with proteolytic maturation occurring only in the budding virion. Mason-Pfizer monkey virus mutants that are defective in plasma membrane targeting, accordingly, assemble intracellular immature capsids consisting of uncleaved polyproteins (30, 32). In HIV-1, on the other hand, significant cleavage of Gag also occurs in the cytoplasm (11), suggesting less tightly controlled PR activation.

Lack of polyprotein cleavage despite assembly and intracellular budding in the case of IAP may therefore be due to a defect in PR function (19) or secondary to aberrant intracellular transport. Interestingly, an IAP-like phenotype of morphogenesis was observed for a deletion mutant of HIV lacking a large internal segment within MA. The resulting particles in the ER were always immature, although they clearly did not have a defect in PR and might have contained at least partially

cleaved core proteins (5, 6). If budding at the plasma membrane or additional factors encountered at this site were determining factors for virus maturation, one would expect that redirection of MIA-14 polyproteins to the cell surface should be sufficient to initiate proteolysis. Specific cleavage was indeed observed for a chimeric polyprotein containing the plasma membrane-targeting signal of the Src protein (MIA-4), which also led to release of extracellular virus. Cleavage was more complete in the particle fraction and was specifically mediated by the viral PR. Furthermore, cleavage of an in vitro-translated Gag polyprotein with bacterially expressed IAP PR yielded proteins identical in mobility to those observed in extracellular particles. Thus, at least in the experimental system presented here, retroviral particle assembly can occur at almost any location within the cell, while polyprotein processing and, consequently, virion maturation are confined to a specific cellular site: the plasma membrane.

Most of the numerous IAP elements in the mouse genome carry large deletions and are clearly defective (reviewed in reference 19). Nevertheless, occasional transposition of IAP elements into new locations has been observed with a low frequency (9, 19). Retrotransposition of IAPs occurs through an RNA intermediate in a mechanism which appears not to include an extracellular phase (9, 19). Since IAP polyproteins are uncleaved and the particle-associated reverse transcriptase activity is low compared to that of murine leukemia virus (reviewed in reference 19), the defect in IAP replication may be due to lack of PR activity. In this case, occasional new insertions into the host cell genome may be caused by rare particles, able to cleave the polyprotein and mature the viral capsid, which need to escape from the ER and subsequently deliver the viral cDNA to the nucleus. These particles may, then, account for the rare events of reverse transcription and integration at novel sites, while the vast majority of IAPs remain immature and do not contribute to transposition. Our data indicate that IAP proteolysis can indeed be activated, and it is conceivable, therefore, that PR activation is required for transfer of IAP elements to new genomic locations, analogous to regular retroviral replication. Alternatively, this transfer may occur independently of PR activation by atypical reverse transcription of the RNA genome and integration into chromosomal DNA.

The results of this study address a general enigma of retroviral replication. If viral polyproteins contain an active PR sequence, why is proteolysis confined to the nascent virion and how is PR activation triggered? Since PR is encoded as a monomeric subunit and is active only as a dimer, concentration-dependent dimerization may be one determining factor. Consistent with this hypothesis, expression of a genetically linked PR dimer as part of retroviral polyproteins induced premature PR activation and loss of particle formation (2, 15). Local concentration at the assembly site cannot be the sole determinant, however, since the type D, IAP, or chimeric polyproteins analyzed in this study are capable of assembling intracellular capsids or capsid-like particles yet remain uncleaved within these particles. Our results indicate that a factor restricted to the plasma membrane is required for PR activation, at least in this experimental system. The identity of this factor is unknown, although several options seem possible: activation of PR by cellular or viral cofactors or by posttranslational modification at the plasma membrane, relief of inactivation, or environmental changes provided, e.g., by the lipid or protein composition of the membrane acquired during envelopment or by the extracellular milieu. Alternatively, triggering of proteolysis could be due to conformational alteration of the polyprotein substrate rather than to regulation of PR itself. Processing may be restricted by inaccessibility of cleavage sites, leading to stable polyproteins, despite an active PR, which are rendered cleavable only upon transport of the polyprotein to the plasma membrane. The experimental system described in this report provides a valuable tool for analysis of these possibilities and identification and characterization of a viral and/or cellular factor(s) required for retrovirus maturation and infectivity.

ACKNOWLEDGMENTS

We are grateful to K. Lueders for providing MIA-14 cDNA and anti-IAP Gag serum, to M. Pawlita for providing a CMV expression vector, to E. Hunter for suggestions and discussion, and to J. Konvalinka for suggestions concerning PR expression. We thank A.-M. Heuser for performing the initial cloning and expression experiments and H. Spring and J. Bridger for help with the confocal immunofluorescence micrographs.

This work was supported in part by a grant from the German Ministry for Research and Technology to H.-G.K.

REFERENCES

1. **Bennett, R. P., T. D. Nelle, and J. W. Wills.** 1993. Functional chimeras of the Rous sarcoma virus and human immunodeficiency virus Gag proteins. J. Virol. **67:**6487–6498.
2. **Burstein, H., D. Bizub, and A. M. Skalka.** 1991. Assembly and processing of avian retroviral *gag* polyproteins containing linked protease dimers. J. Virol. **65:**6165–6172.
3. **Campbell, S., and V. M. Vogt.** 1995. Self-assembly in vitro of purified CA-NC proteins from Rous sarcoma virus and human immunodeficiency virus type 1. J. Virol. **69:**6487–6497.
4. **Chen, C., and H. Okayama.** 1987. High-efficiency transformation of mammalian cells by plasmid DNA. Mol. Cell. Biol. **7:**2745–2752.
5. **Fäcke, M., A. Janetzko, R. L. Shoeman, and H.-G. Kräusslich.** 1993. A large deletion in the matrix domain of the human immunodeficiency virus *gag* gene redirects virus particle assembly from the plasma membrane to the endoplasmic reticulum. J. Virol. **67:**4972–4980.
6. **Gallina, A., G. Mantoan, G. Rindi, and G. Milanesi.** 1994. Influence of MA internal sequences, but not of the myristylated N-terminus sequence, on the binding site of HIV-1 Gag protein. Biochem. Biophys. Res. Commun. **204:** 1031–1038.
7. **Gelderblom, H. R., E. H. Hausmann, M. Özel, G. Pauli, and M. A. Koch.** 1987. Fine structure of human immunodeficiency virus (HIV) and immunolocalization of structural proteins. Virology **156:**171–176.
8. **Gheysen, D., E. Jacobs, F. de Foresta, C. Thiriart, M. Francotte, D. Thines, and M. De Wilde.** 1989. Assembly and release of HIV 1 precursor Pr55gag virus like particles from recombinant baculovirus infected insect cells. Cell **59:**103–112.
9. **Heidmann, O., and T. Heidmann.** 1991. Retrotransposition of a mouse IAP sequence tagged with an indicator gene. Cell **64:**159–170.
10. **Jones, T. A., G. Blaug, M. Hansen, and E. Barklis.** 1990. Assembly of *gag*-β-galactosidase fusion proteins into retrovirus particles. J. Virol. **64:** 2265–2279.
11. **Kaplan, A. H., and R. Swanstrom.** 1991. Human immunodeficiency virus type 1 Gag proteins are processed in two cellular compartments. Proc. Natl. Acad. Sci. USA **88:**4528–4532.
12. **Kaplan, A. H., J. A. Zack, M. Knigge, D. A. Paul, D. J. Kempf, D. W. Norbeck, and R. Swanstrom.** 1993. Partial inhibition of the human immunodeficiency virus type 1 protease results in aberrant virus assembly and the formation of noninfectious particles. J. Virol. **67:**4050–4055.
13. **Klikova, M., S. S. Rhee, E. Hunter, and T. Ruml.** 1995. Efficient in vivo and in vitro assembly of retroviral capsids from Gag precursor proteins expressed in bacteria. J. Virol. **69:**1093–1098.
14. **Kohl, N. E., E. A. Emini, W. A. Schleif, L. J. Davis, J. C. Heimbach, R. A. F. Dixon, E. M. Scolnick, and I. S. Sigal.** 1988. Active human immunodeficiency virus protease is required for viral infectivity. Proc. Natl. Acad. Sci. USA **85:**4686–4690.
15. **Kräusslich, H.-G.** 1991. Human immunodeficiency virus proteinase dimer as component of the viral polyprotein prevents particle assembly and viral infectivity. Proc. Natl. Acad. Sci. USA **88:**3213–3217.
16. **Kräusslich, H.-G.** 1992. Specific inhibitor of human immunodeficiency virus proteinase prevents the cytotoxic effects of a single-chain proteinase dimer and restores particle formation. J. Virol. **66:**567–572.
17. **Kräusslich, H.-G., and R. Welker.** 1996. Intracellular transport of retroviral capsid components. Curr. Top. Microbiol. Immunol. **214:**25–64.
18. **Kräusslich, H.-G., H. Schneider, G. Zybarth, C. A. Carter, and E. Wimmer.** 1988. Processing of in vitro-synthesized *gag* precursor proteins of human immunodeficiency virus (HIV) type 1 by HIV proteinase generated in *Escherichia coli*. J. Virol. **62:**4393–4397.

19. **Kuff, E. L., and K. K. Lueders.** 1988. The intracisternal A particle gene family: structure and functional aspects. Adv. Cancer Res. **51:**183–276.
20. **Kunkel, T. A.** 1985. Rapid and efficient site-directed mutagenesis without phenotypic selection. Proc. Natl. Acad. Sci. USA **82:**488–492.
21. **Marciani, D. J., and E. L. Kuff.** 1973. Isolation and partial characterization of the internal structural proteins from murine intracisternal A particles. Biochemistry **12:**5075–5083.
22. **McDonald, K.** 1984. Osmium ferricyanide fixation improves microfilament preservation and membrane vesiculation in a variety of animal cell types. J. Ultrastruct. Res. **86:**107–118.
23. **Mergener, K., M. Fäcke, R. Welker, V. Brinkmann, H. R. Gelderblom, and H.-G. Kräusslich.** 1992. Analysis of HIV particle formation using transient expression of subviral constructs in mammalian cells. Virology **186:**25–39.
24. **Mietz, J. A., Z. Grossman, K. K. Lueders, and E. L. Kuff.** 1987. Nucleotide sequence of a complete mouse intracisternal A-particle genome: relationship to known aspects of particle assembly and function. J. Virol. **61:**3020–3029.
25. **Nermut, M. V., and D. J. Hockley.** 1996. Comparative morphology and structural classification of retroviruses. Curr. Top. Microbiol. Immunol. **214:** 1–24.
26. **Ono, M., H. Toh, T. Miyata, and T. Awaya.** 1985. Nucleotide sequence of the Syrian hamster intracisternal A-particle gene: close evolutionary relationship of type A particle gene to type B and D oncovirus genes. J. Virol. **55:**387–394.
27. **Pellman, D., F. R. Garber, F. R. Cross, and H. Hanafusa.** 1985. An N-terminal peptide from $p60^{src}$ can direct myristoylation and plasma membrane localization when fused to heterologous proteins. Nature **314:**374–377.
28. **Pepinsky, R. B., and V. M. Vogt.** 1979. Identification of retrovirus matrix proteins by lipid protein cross-linking. J. Mol. Biol. **131:**819–837.
29. **Pepinsky, R. B., and V. M. Vogt.** 1984. Fine-structure analyses of lipid-protein and protein-protein interactions of *gag* protein p19 of the avian sarcoma and leukemia viruses by cyanogen bromide mapping. J. Virol. **52:** 145–153.
30. **Rhee, S. S., and E. Hunter.** 1987. Myristylation is required for intracellular transport but not for assembly of D-type retrovirus capsids. J. Virol. **61:**1045–1053.
31. **Rhee, S. S., and E. Hunter.** 1990. A single amino acid substitution within the matrix protein of a type D retrovirus converts its morphogenesis to that of a type C retrovirus. Cell **63:**77–86.
32. **Rhee, S. S., and E. Hunter.** 1991. Amino acid substitutions within the matrix protein of type D retroviruses affect assembly, transport and membrane association of a capsid. EMBO J. **10:**535–546.
33. **Roberts, N. A., J. A. Martin, D. Kinchington, A. V. Broadhurst, J. C. Craig, I. B. Duncan, S. A. Galpin, B. K. Handa, J. Kay, A. Kröhn, R. W. Lambert, J. H. Merrett, J. S. Mills, K. E. B. Parkes, S. Redshaw, A. J. Ritchie, D. L. Taylor, G. J. Thomas, and P. J. Machin.** 1990. Rational design of peptide-based HIV-proteinase inhibitors. Science **248:**358–361.
34. **Sakalian, M., S. D. Parker, R. A. Weldon, Jr., and E. Hunter.** 1996. Synthesis and assembly of retrovirus Gag precursors into immature capsids. J. Virol. **70:**3706–3715.
35. **Sambrook, J., E. F. Fritsch, and T. Maniatis.** 1989. Molecular cloning: a laboratory manual, 2nd ed. Cold Spring Harbor Laboratory Press, Cold Spring Harbor, N.Y.
36. **Studier, F. W., and B. A. Moffat.** 1986. Use of bacteriophage T7 RNA polymerase to direct selective high-level expression of cloned genes. J. Mol. Biol. **189:**113–130.
37. **Vogt, V. M.** 1996. Proteolytic processing and particle maturation. Curr. Top. Microbiol. Immunol. **214:**95–132.
38. **Wang, C. T., J. Stegeman-Olsen, Y. Zhang, and E. Barklis.** 1994. Assembly of HIV GAG-betagalactosidase fusion proteins into virus particles. Virology **200:**524–534.
39. **Weldon, R. A., Jr., C. R. Erdie, M. G. Oliver, and J. W. Wills.** 1990. Incorporation of chimeric Gag protein into retroviral particles. J. Virol. **64:**4169–4179.
40. **Welker, R., and H. G. Kräusslich.** Unpublished data.
41. **Wills, J. W., R. C. Craven, and J. A. Achacoso.** 1989. Creation and expression of myristylated forms of Rous sarcoma virus Gag protein in mammalian cells. J. Virol. **63:**4331–4343.
42. **Zhou, W., L. J. Parent, J. W. Wills, and M. D. Resh.** 1994. Identification of a membrane-binding domain within the amino-terminal region of human immunodeficiency virus type 1 Gag protein which interacts with acidic phospholipids. J. Virol. **68:**2556–2569.